ROSS
ENGINEERING
Engineering Services

# Finite Element Stress Analysis of

# Icosahedron Beam

## Job # 05-006

## Prepared for:

## Mr. Sam Lanahan
## Flextegrity


**Abstract**

This is a stress analysis report for the Icosahedron Beam. The analysis was performed to compare a beam constructed of the Icosahedrons fabricated of Aluminum to a standard Wood beam. The predicted deflections are similar, while the component stresses in the Icosahedron beam are generally low. The finite element analyses were performed using Cosmos/M from Structural Research Analysis Corporation.


September 29, 2005


P.O. Box 65322 University Place, WA, 98464-1322 (253) 858-2575

# Objective

This simulation was performed to compare the deflections in the proposed icosahedron beam to that of a solid wood beam of the same nominal dimensions. The geometry provided was scaled to approximately 92% in order to approximate the net dimensions of a nominal 4" x 6" beam (3.5" x 5.5"). This resulted in a beam with a 3.5" x 5.58" cross section.

**Loading** - Applied Load - The applied load of 250 lbf/ft is a round number (1000 lbf/4 ft) which produces a bending deflection near 1/360th of the span for the wooden beam around one axis. The maximum deflection of 1/360th of the span is a common design value for beams in the building trades. The same load was applied to both beams in both directions to make comparison easier.

# Definitions:

**Strong Axis** - Parallel to the larger moment of inertia of the wood beam. This corresponds to the larger (5.58") beam dimension.

**Weak Axis** - Perpendicular to the Strong Axis.

**Von Mises Stress** - Common name for one Total Energy theory (Maximum Distortion Energy). Materials generally fail in shear, but the standard test method is a tensile test. Using Von Mises stress allows the calculated stress to be compared with the measured (tested) tensile yield stress for a material.

# Summary & Conclusions:

The predicted stress in the beam during weak axis bending locally exceed yield. This would cause local yielding and load redistribution in use, but is at least partly due to the method of load application. In strong axis bending, where the load had a larger area to be applied, the predicted stress is everywhere less than yield.

The predicted deflections were similar to the nominal wood beam. Predicted deflections were 0.493 in.(case 1) & 0.757 in. (case 2) vs. 0.64 in - weak axis and 0.079 in. vs. 0.25 in. - strong axis for the modeled and wooden beams respectively.

# Assumptions

The analysis was performed using a shell surface model that represents the mid-plane of the part.

Only one half of the total length of the beam was modeled and symmetry at the center of the span was used. No other symmetry was used in modeling the beam because there were no other symmetry axes available.

The use of symmetry in analysis is common and is used to make a model a more manageable size. Symmetry is dependent on both part geometry and loading conditions. For this geometry and loading, the only axis of symmetry was located at the center of the beam.

The symmetry boundary conditions applied at the beam center cause a moment to be applied at the beam center. This beam configuration is classified as simply supported and guided. As stated above, the beam length is one half of the simply supported beam or 4 feet. Comparing the closed form solutions for a simply supported beam and a simple-guided beam of 1/2 the simply supported beams' length, it will be seen that the calculated deflections for the two cases are the same.



ROSS ENGINEERING P.O. Box 65322 University Place, WA 98464-1322

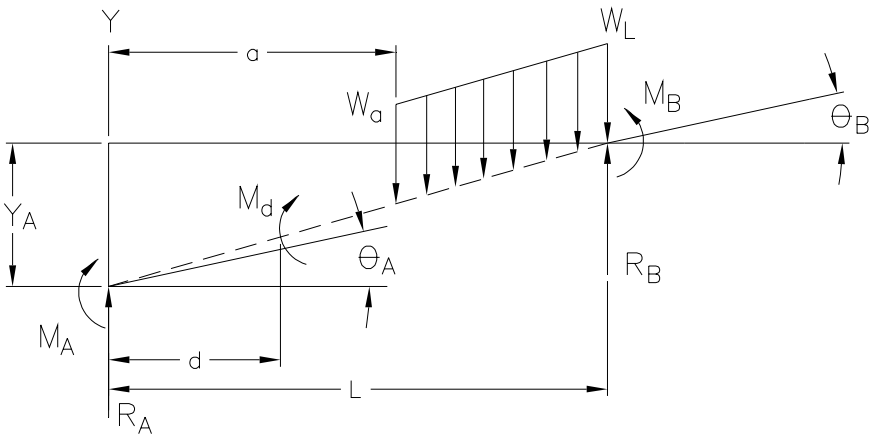


**Figure 1 Plot Showing General Beam Notation**

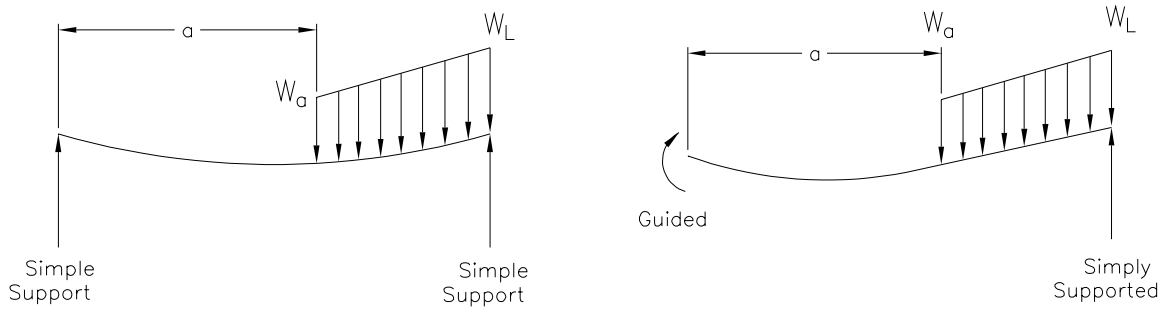


**Figure 2 Plot of Specific Beam Boundary Conditions**

Figures 1 and 2 show the general notation and the specific beam supports used in the beam analysis. For the cases evaluated in this report, $w_a = w_L$ and a = 0 and we thus have a uniform load on the entire span. The deflection equations for the two cases are shown below and the calculated deflections are compared.

For a simply supported beam with a uniform load, the deflection may be found from:

$$\delta_{\max_{simple}} = \frac{-5 w_a \, l^4}{384 \, EI}$$

where, $\delta_{\max} \equiv Maximum\ Deflection$

$w_a \equiv Uniform\ Load\ (Force/unit\ length)$

$l \equiv length$

$E \equiv Modulus\ of\ Elasticity$

$I \equiv Moment\ of\ Inertia$

And for a simple-guided beam, the deflection may be found from:

$$\delta_{\max_{s-g}} = \frac{-5 w_a \, l^4}{24 \, EI}$$

Both beams have the same cross-section properties and Modulus of Elasticity. The simple-guided beam is one half the length of the simply supported beam and



ROSS ENGINEERING P.O. Box 65322 University Place, WA 98464-1322

$$\delta_{\max_{s-g}} = \frac{-5w_a\left(\frac{l_{simple}}{2}\right)^4}{24\,EI} = \frac{-5w_a \times \frac{(l_{simple})^4}{16}}{24\,EI} = \frac{-5w_a\,(l_{simple})^4}{16 \times 24\,EI} = \frac{-5w_a\,(l_{simple})^4}{384\,EI}$$

,therefore, the deflections for the half symmetric beam and the simply supported beam will be the same for beams given the same cross section and material and the assumption of symmetry is valid.

# Discussion of Analysis Details

Two load cases were run on the model for the two major axes of the beam, one was for bending about the weak axis (the 3.5 in. dimension) and the other about the strong axis (5.58 in. dimension.

The part model was generated form the geometry provided, except the sizes were scaled to approximately 92% to provide a 3.5 in. width. The geometry was scaled around both axes resulting in a depth of 5.58 in. The applied load was 250 lbf/ft. in all cases.

The same 3.5" x 5.58" cross section was used to calculate the deflections of a wood beam. The properties for the wooden beam were those of Structural Select grade with a modulus of elasticity of $1.8 \times 10^6$ psi. The corresponding modulus for 6061-T6 Aluminum was $10 \times 10^6$ psi.

Two sets of displacement boundary conditions were used. The initial set over constrained the beam from twisting, increasing the predicted stress adjacent to the applied constraints. When the additional constraints were removed, the beam was allowed to twist more easily, this also allowed the deflections to increase. This effect was only present in the weak axis bending case and is due to the asymmetric geometry. Changing the geometry for a more symmetric beam will reduce the twist and should reduce the deflections.

The aluminum icosahedron beam modeled in the finite element model weighs approximately 3.13 lbf/ft. using an aluminum density of 0.097 lb/in$^3$. This is a 21% reduction from the wood beam of the same dimensions assuming a wood density of 0.017 lb/in$^3$. which corresponds to a specific gravity of 0.9. The weight reduction could be increased by further reducing the thickness of the icosahedron walls where the stresses are low.



ROSS ENGINEERING P.O. Box 65322 University Place, WA 98464-1322

# Beam Equations:

The dimensions of the Icosahedron beam are 3.5 in x 5.58 in. The same dimensions are used for the comparison wooden beam. To determine the deflections of the wooden beam, the section properties are first determined.

$$I_x = \frac{bh^3}{12} = \frac{3.5\ in \times \left(5.58\ in\right)^3}{12} = 50.7\ in^4$$

$$I_y = \frac{bh^3}{12} = \frac{5.58\ in \times \left(3.5\ in\right)^3}{12} = 19.9\ in^4$$

The section properties, along with the modulus of elasticity are used to calculate the maximum deflection, which occurs at the center of the beam. The maximum deflections are found from [Roark's]:

$$y_{\max_{strong}} = -\frac{5 \times w_a \times L^4}{384 EI} = -\frac{5 \times 250\ \frac{lbf}{ft} \times \frac{ft}{12\ in} \times \left(96\ in\right)^4}{384 \times 1.8 \times 10^6\ psi \times 50.7\ in^4} = -0.0505\ in$$

$$y_{\max_{weakg}} = -\frac{5 \times w_a \times L^4}{384 EI} = -\frac{5 \times 250\ \frac{lbf}{ft} \times \frac{ft}{12\ in} \times \left(96\ in\right)^4}{384 \times 1.8 \times 10^6\ psi \times 19.9\ in^4} = -0.129\ in$$

where:

$E \equiv 1.8 \times 10^6\ psi$ – Structural Select

$w_a \equiv 250 \frac{lbf}{ft}$ – Unit Load

Using these relations, the equivalent moment of inertia for the Icosahedron beam may be calculated, based on the predicted deflection:

$$y_{\max_{ICO-weak}} = -\frac{5 \times 250 \frac{lbf}{ft} \times \frac{ft}{12in} \times \left(96in\right)^4}{384 \times 10 \times 10^6\ psi \times I_{ICO_{weak}}} = -0.757\ in \Rightarrow$$

$$I_{ICO_{weak}} = \frac{5 \times 250 \frac{lbf}{ft} \times \frac{ft}{12in} \times \left(96in\right)^4}{384 \times 10 \times 10^6\ psi \times 0.493in} = 3.04\ in^4$$

$$I_{ICO_{strong}} = \frac{5 \times 250 \frac{lbf}{ft} \times \frac{ft}{12in} \times \left(96in\right)^4}{384 \times 10 \times 10^6\ psi \times 0.079in} = 29.165\ in^4$$

These equivalent moments of inertia could be used to calculate stresses and deflections for different beam configurations, cantilever, concentrated load, etc. The equivalent modulii would need to be calculated for each beam geometry because scaling is not expected.



ROSS ENGINEERING P.O. Box 65322 University Place, WA 98464-1322

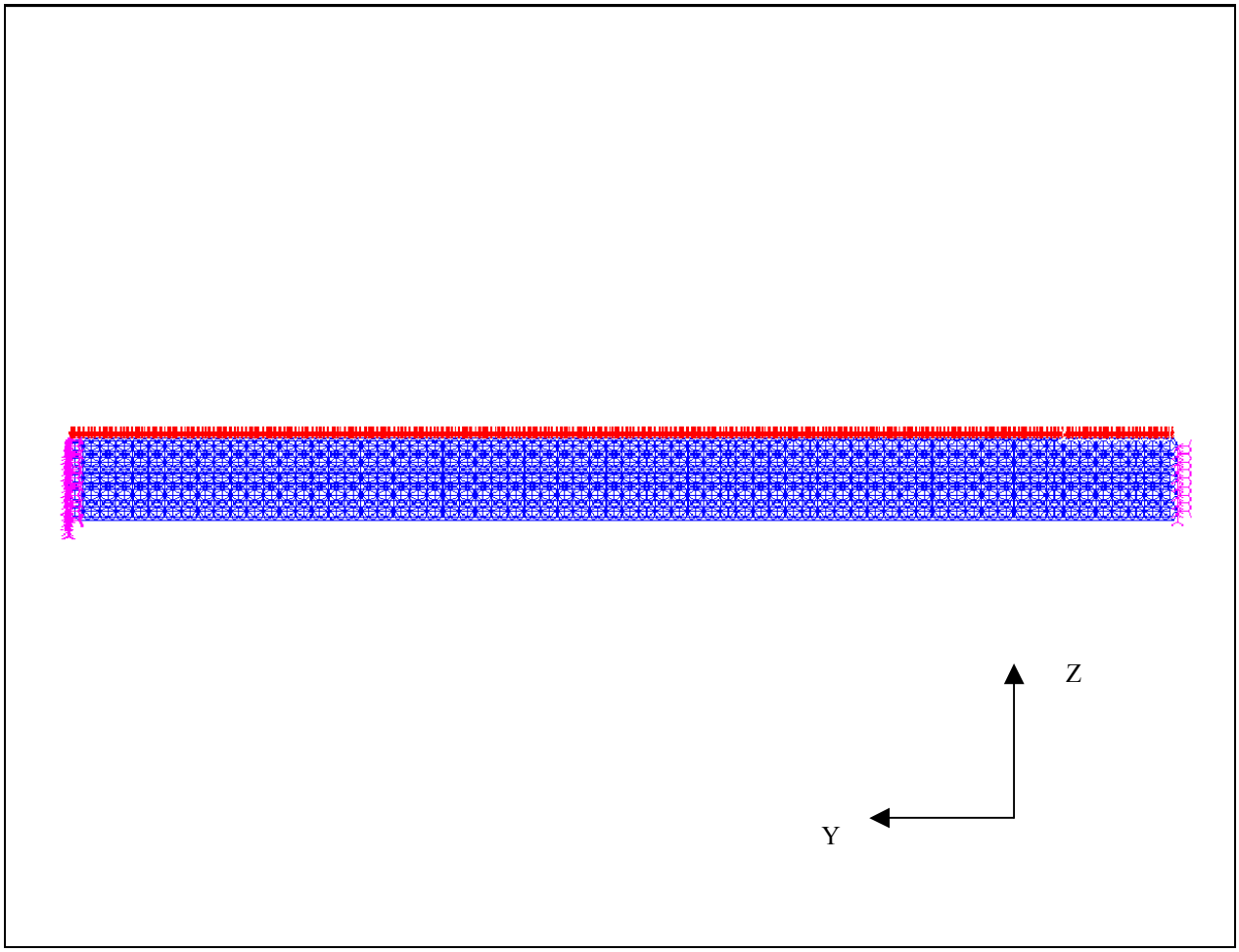


**Figure 3 Plot of Model with Boundary Conditions - Weak Axis - Case 1**

The Figure above shows a plot of the model with the applied boundary conditions. The displacement constraints are shown with the purple arrows and the applied pressure with the red arrows.

One half of the beam length (4 feet) was modeled with symmetry constraints applied at the center (left end). The symmetry constraints consist of rotation constraints about the X - axis applied to the nodes at the left end of the above figure.

The applied load was 250 lbf./ft.

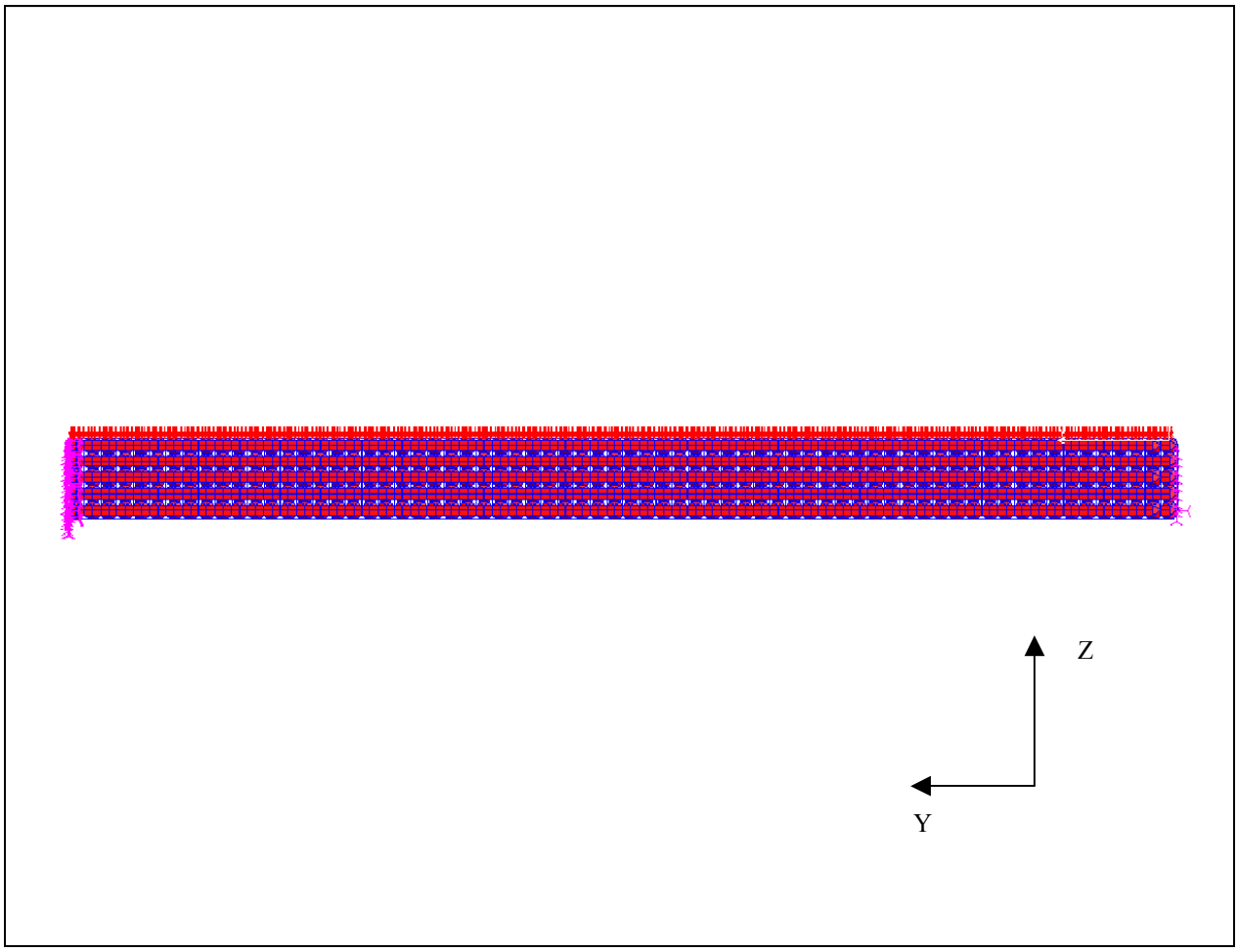


**Figure 4 Plot of Model with Boundary Conditions - Weak Axis - Case 2**

The Figure above shows a plot of the model with the applied boundary conditions. The displacement constraints are shown with the purple arrows and the applied pressure with the red arrows.

The displacement constraints in the axial direction on the right end of the beam, except in the lower right corner, were removed for this case.



ROSS ENGINEERING P.O. Box 65322 University Place, WA 98464-1322

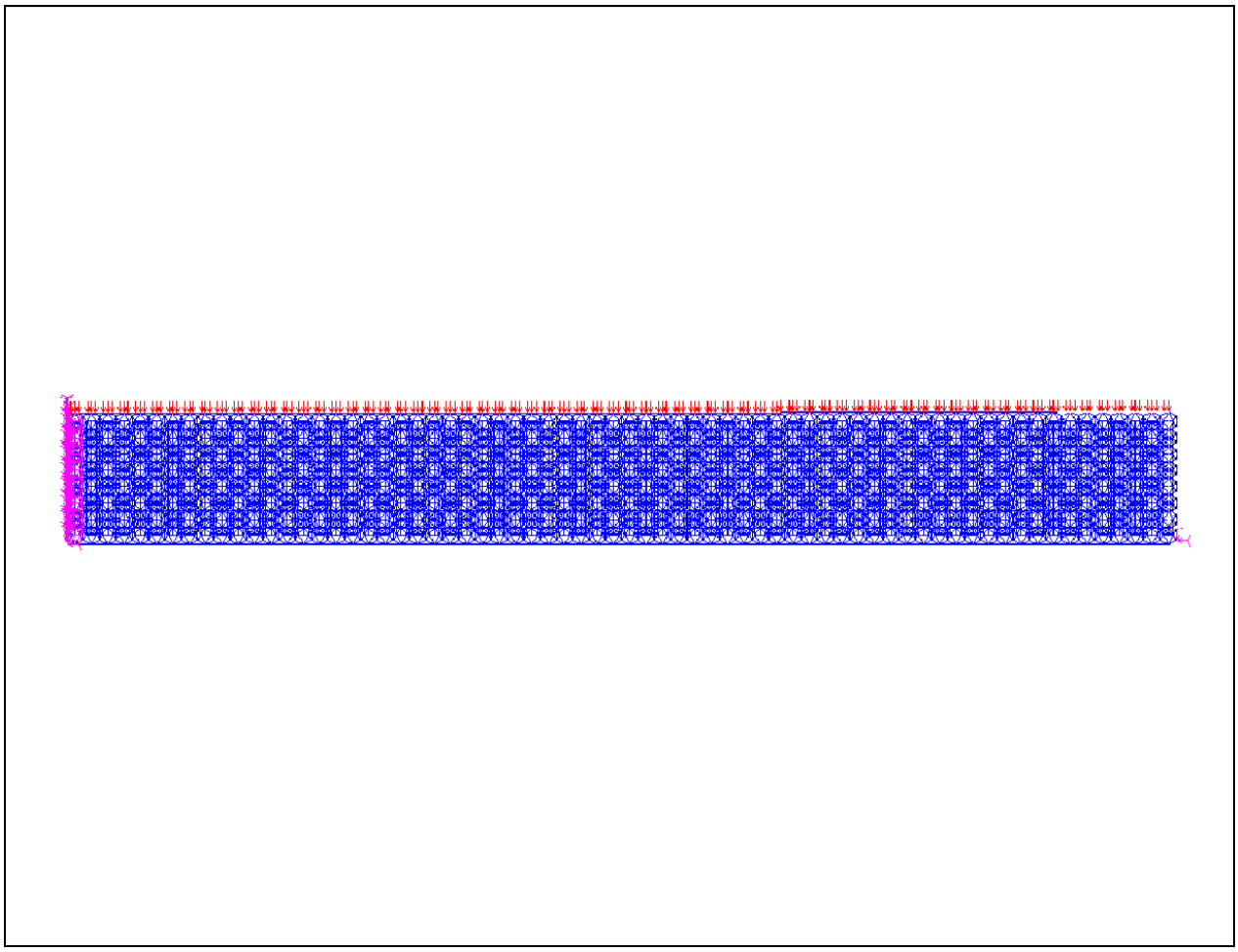

**Figure 5 Plot of Model with Boundary Conditions - Strong Axis**

The Figure above shows a plot of the model with the applied boundary conditions. The displacement constraints are shown with the purple arrows and the applied pressure with the red arrows.



ROSS ENGINEERING P.O. Box 65322 University Place, WA 98464-1322

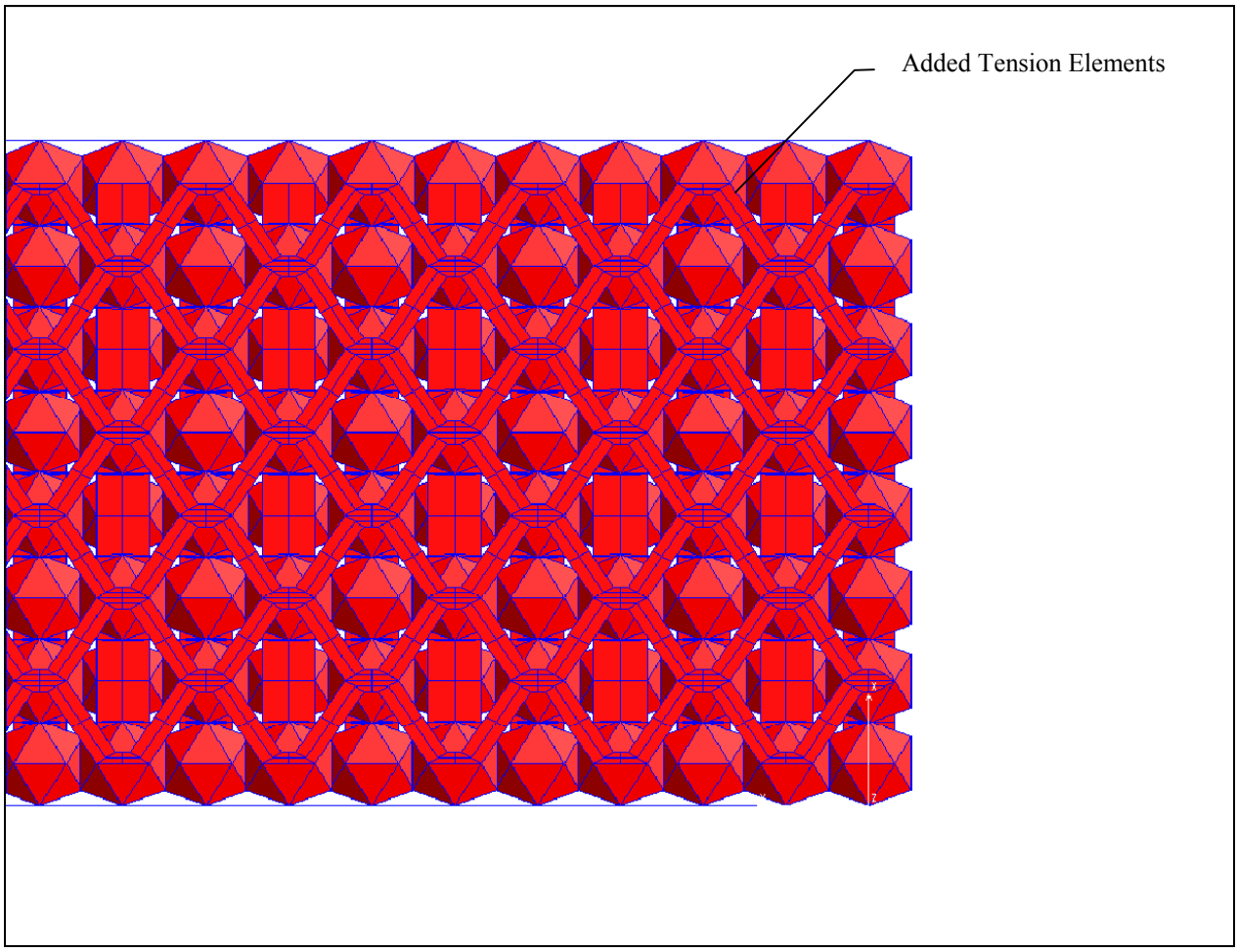


**Figure 6 Plot of Model - Plan View**

The Figure above shows a plot of the model from the top showing the added (top) tension elements. The additional elements were added symmetrically.



ROSS ENGINEERING P.O. Box 65322 University Place, WA 98464-1322

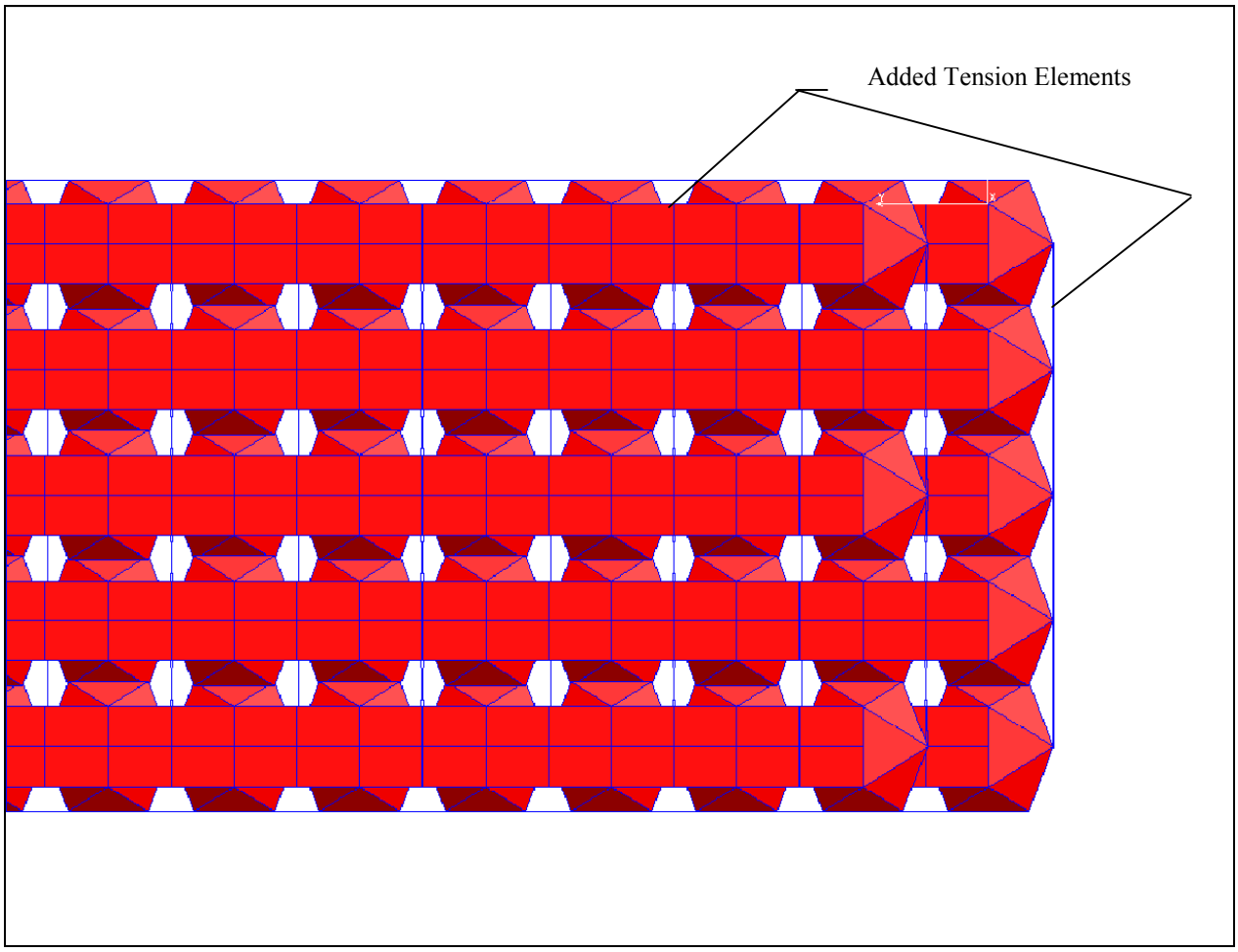


**Figure 7 Plot of Model - Side View**

The Figure above shows a plot of the side view of the model on the simply supported end and showing the added tension elements on the side and end. The additional elements were added symmetrically.



ROSS ENGINEERING P.O. Box 65322 University Place, WA 98464-1322

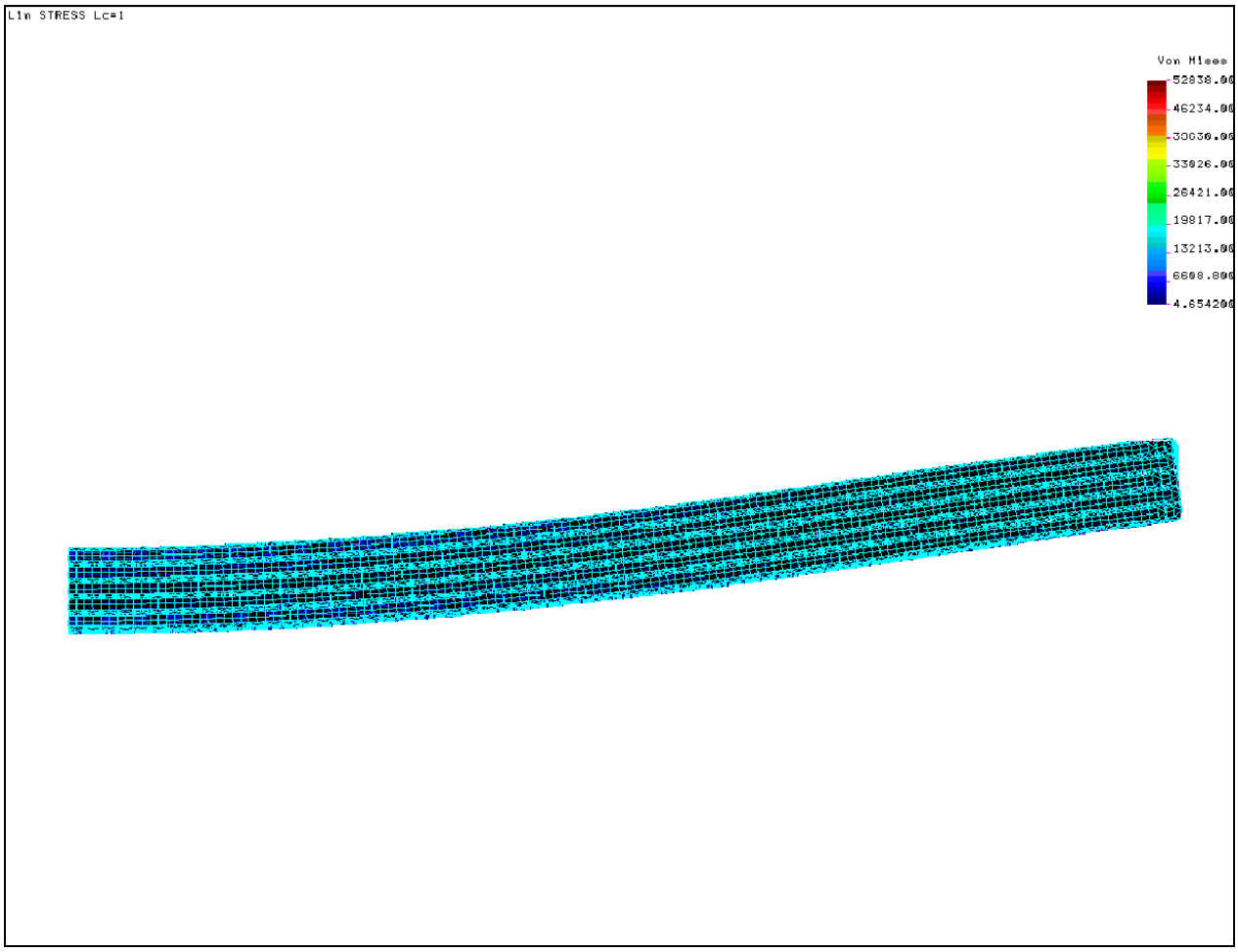


**Figure 8 Plot of Predicted Von Mises Stress - Weak Axis - Case 1**

The Figure above shows a plot of the predicted Von Mises Stress during weak axis bending. The stresses exceeding yield are limited to a few (tension) elements. The maximum stress in the icosahedrons does not exceed yield.



ROSS ENGINEERING P.O. Box 65322 University Place, WA 98464-1322

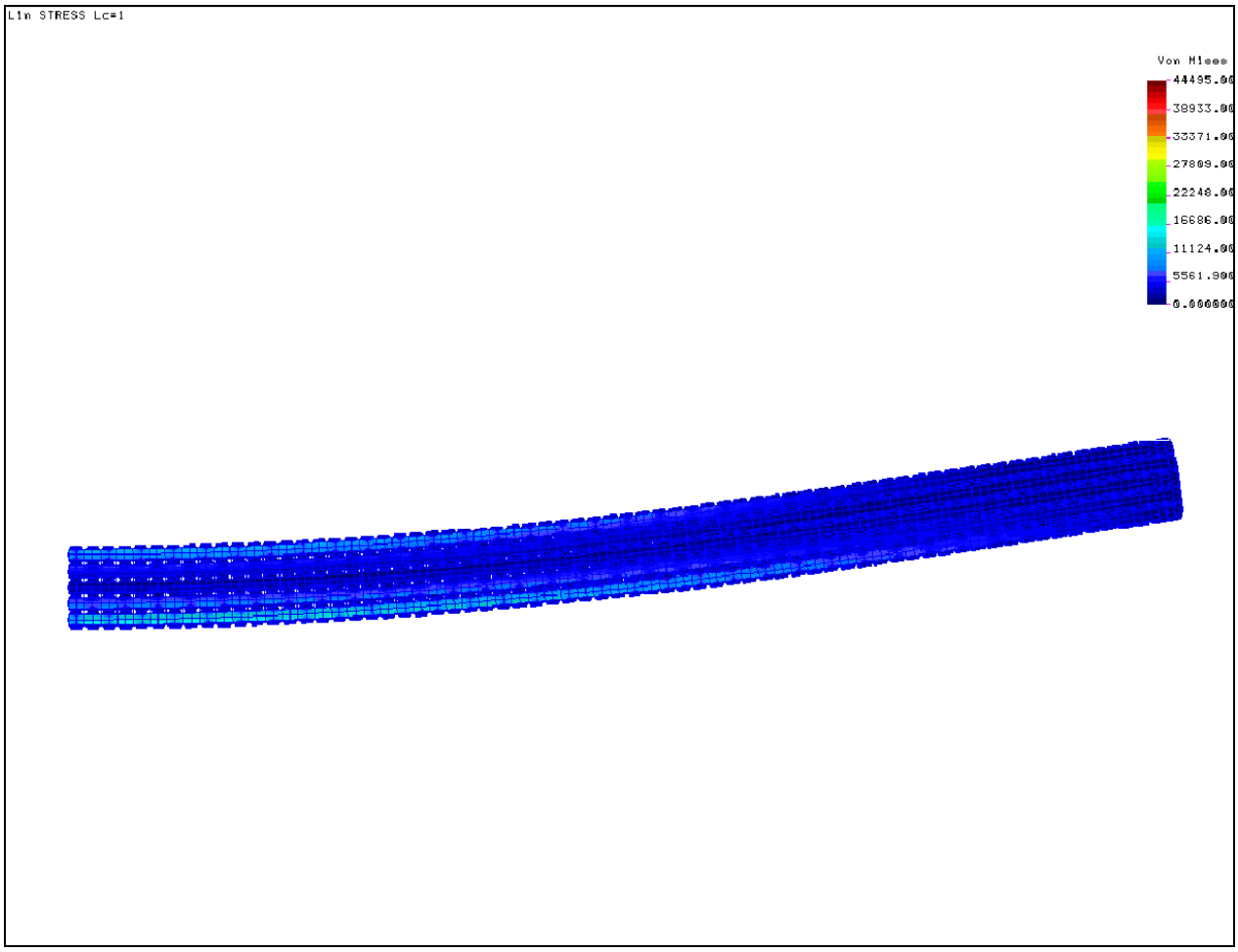


**Figure 9 Plot of Predicted Von Mises Stress - Weak Axis - Case 2**

The Figure above shows a plot of the predicted Von Mises Stress during weak axis bending. The stresses exceeding yield are limited to a few (tension) elements located near the corner displacement constraints (see figure 9). The maximum stress in the icosahedrons does not exceed yield.



ROSS ENGINEERING P.O. Box 65322 University Place, WA 98464-1322

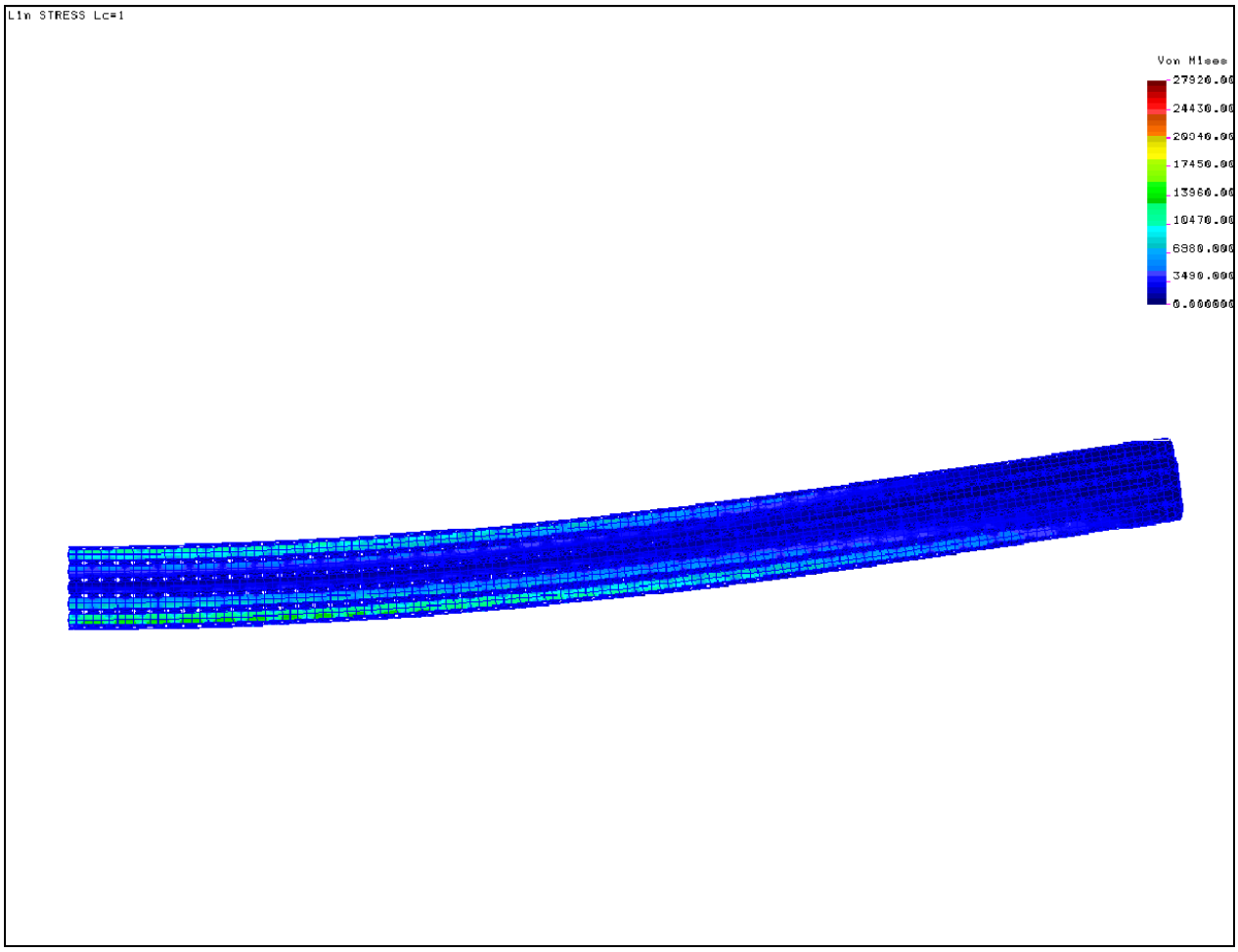


**Figure 10 Plot of Predicted Von Mises Stress - Weak Axis - Case 2 - Scaled**

The Figure above shows a plot of the predicted Von Mises Stress during weak axis bending with the high stress elements at the displacement constraint removed. The elements with stresses exceeding yield were limited to a few elements located near the corner displacement constraints and are shown in figure 9.

The maximum stress in the icosahedrons does not exceed yield.



ROSS ENGINEERING P.O. Box 65322 University Place, WA 98464-1322

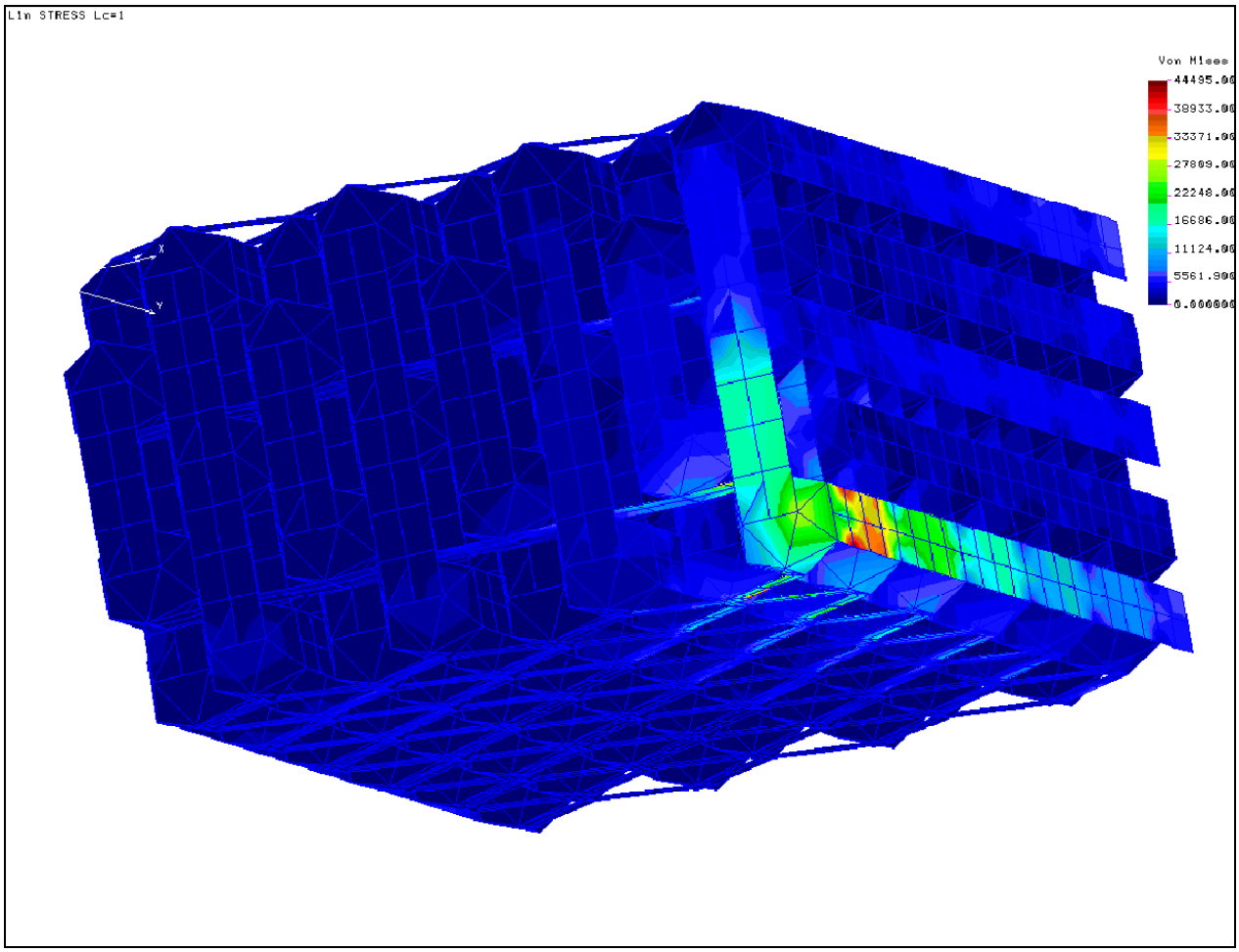


**Figure 11 Plot of Predicted Von Mises Stress - Weak Axis - Case 2 - Constraint Stresses**

The Figure above shows a plot of the predicted Von Mises Stress during weak axis bending rotated to show the high stresses at the displacement constraint. The constraint is required to prevent uncontrolled motion during the analysis but can induce artificial stresses as well as is the case here. With these peak stress elements removed, the stresses throughout the model are more uniform. These stresses are apparently the result of the asymmetry in the model from the uneven number of rows of icosahedrons. This same phenomenon is not evident in the strong axis bending case.



ROSS ENGINEERING P.O. Box 65322 University Place, WA 98464-1322

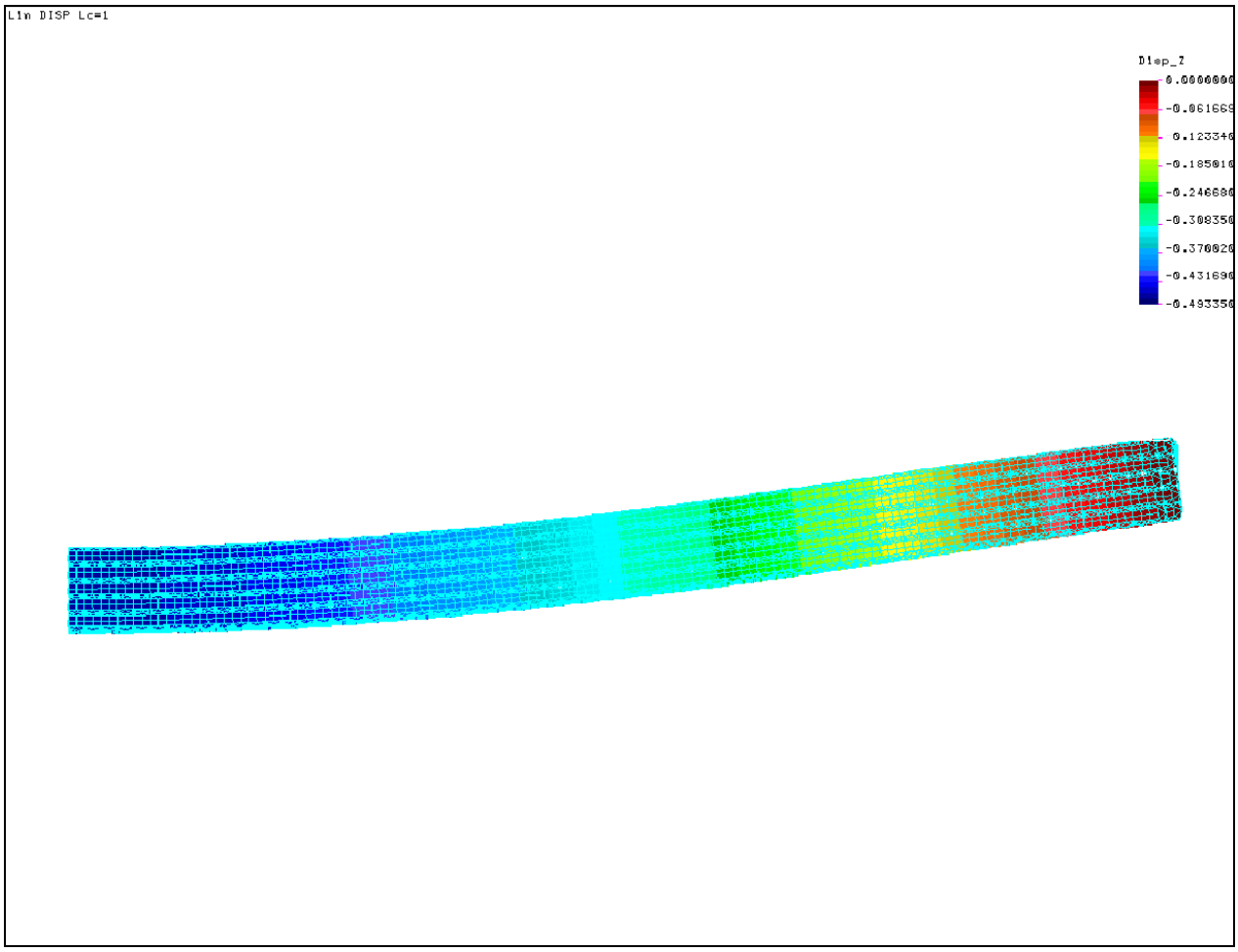


**Figure 12 Plot of Predicted Deflection - Weak Axis - Case 1**

The Figure above shows a plot of the predicted deflection for weak axis bending. The maximum deflection (at the center) is 0.49 in., comparable to that of a solid wood beam.

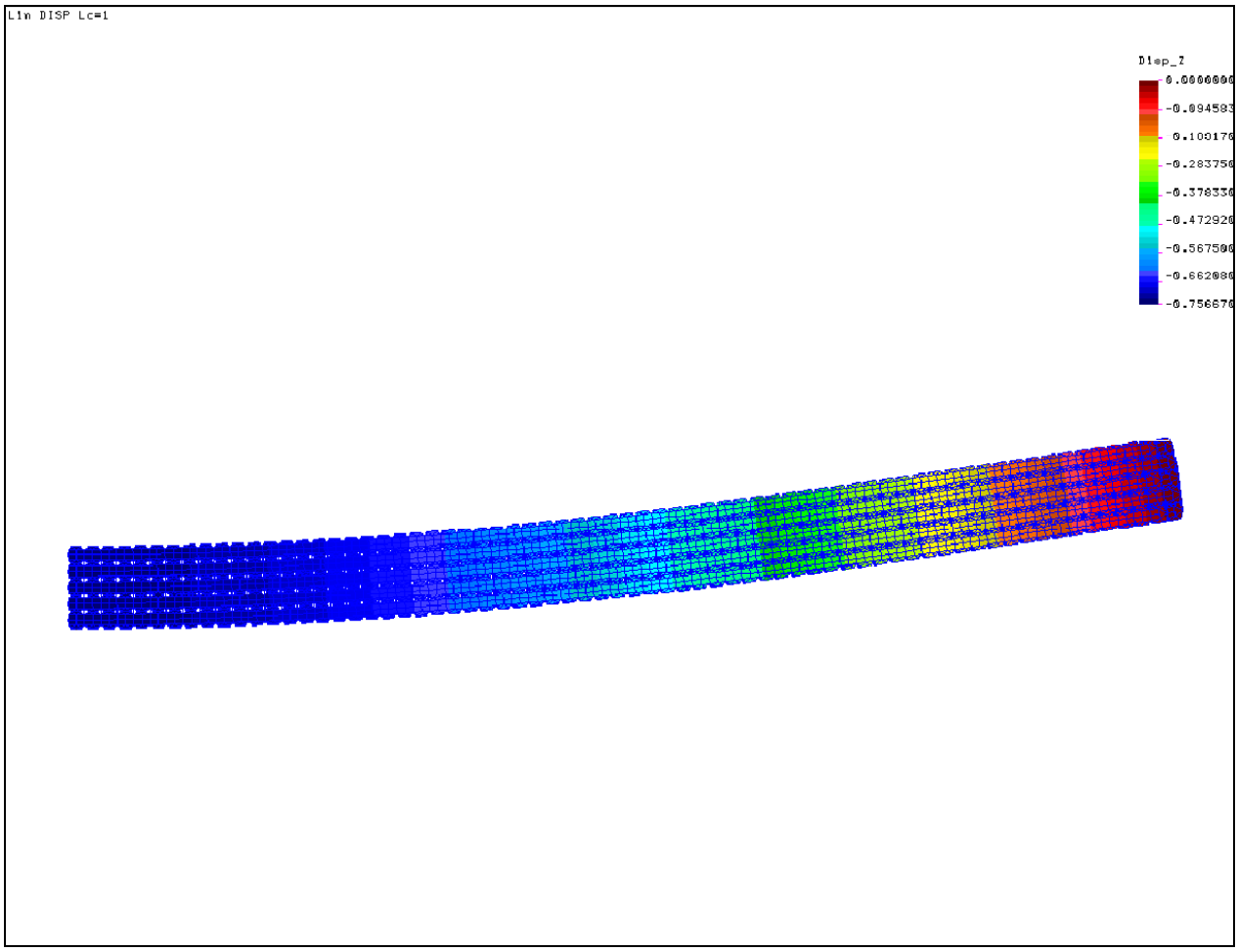


**Figure 13 Plot of Predicted Deflection - Weak Axis - Case 2**

The Figure above shows a plot of the predicted deflection for weak axis bending for case 2. With the beam allowed to twist, the deflections are increased. This twisting would be reduced if not eliminated by adding a diaphragm across the end or by building a more symmetric beam (the model is 5 x 8 icosahedrons). The maximum deflection (at the center) is 0.757 in., comparable to that of a solid wood beam.



ROSS ENGINEERING P.O. Box 65322 University Place, WA 98464-1322

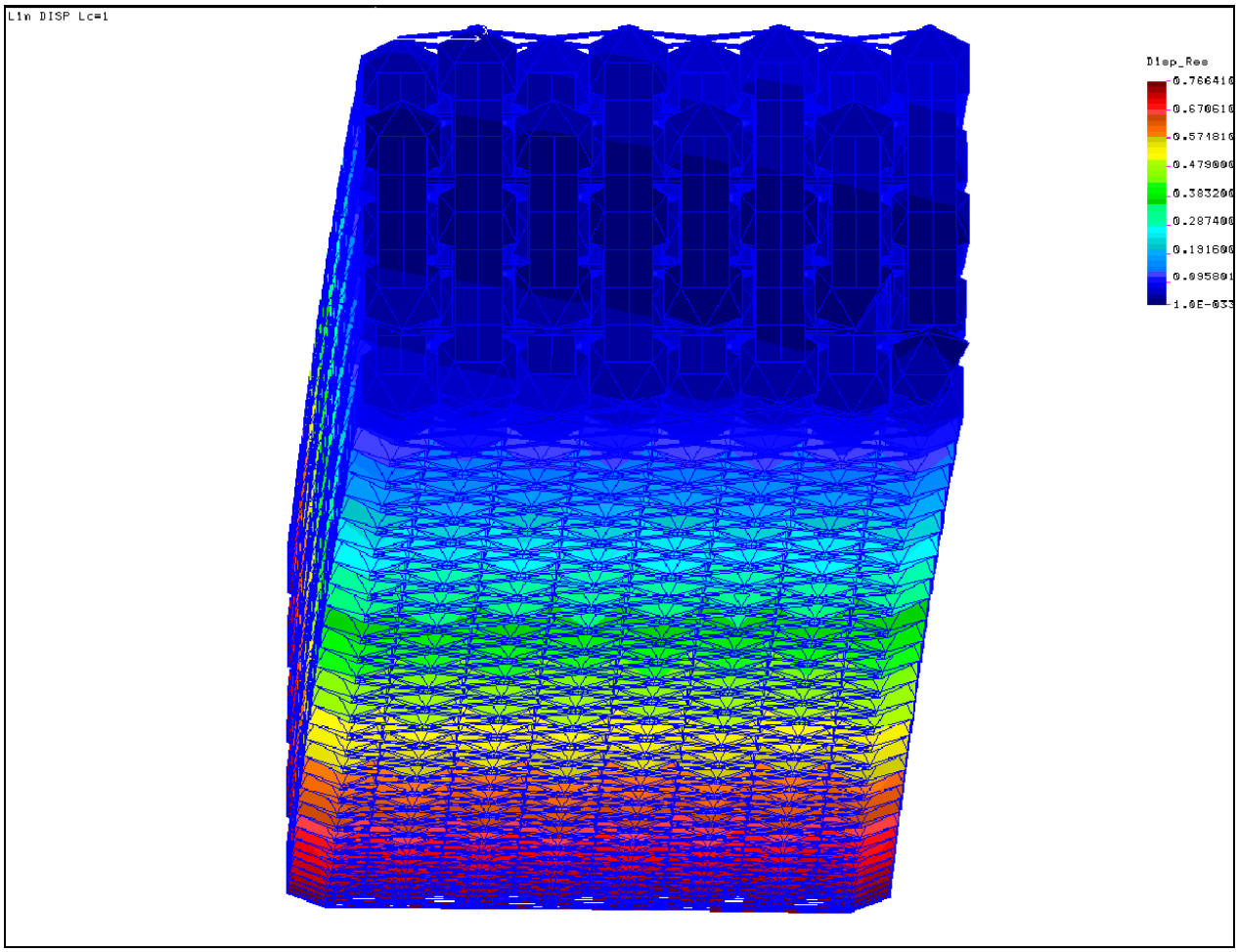


**Figure 14 Plot of Predicted Deflection - Weak Axis - Case 2 - End View**

The Figure above shows a plot of the predicted deflection for weak axis bending for case 2. This plot shows an end view of the beam to illustrate the twist during deflection. The twist is most easily discerned by looking at the lower edge of the plot.

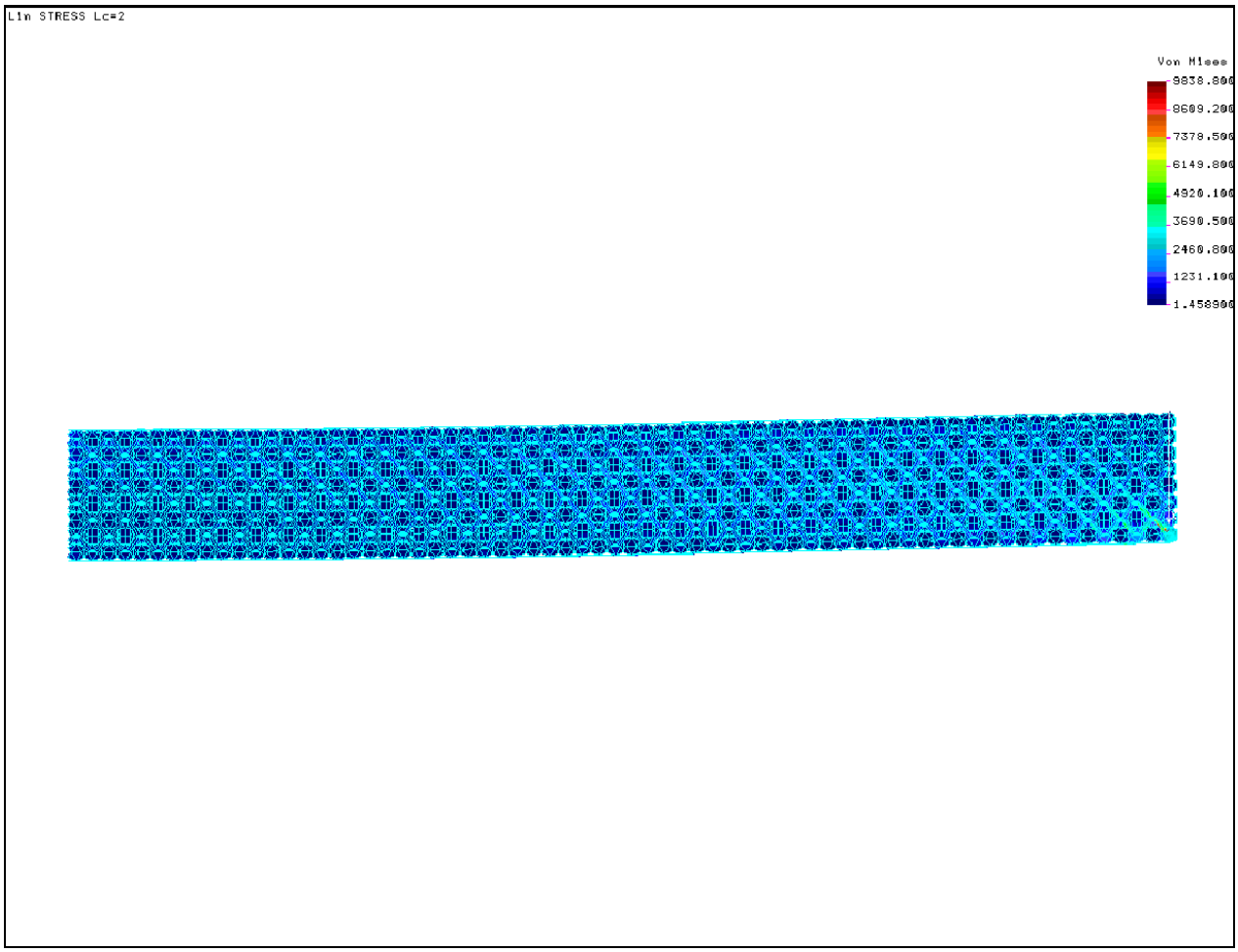


**Figure 15 Plot of Predicted Von Mises Stress - Strong Axis**

The Figure above shows a plot of the predicted Von Mises stress during strong axis bending. Nowhere does the predicted stress exceed yield, mostly due to the increased load application area available in this orientation.

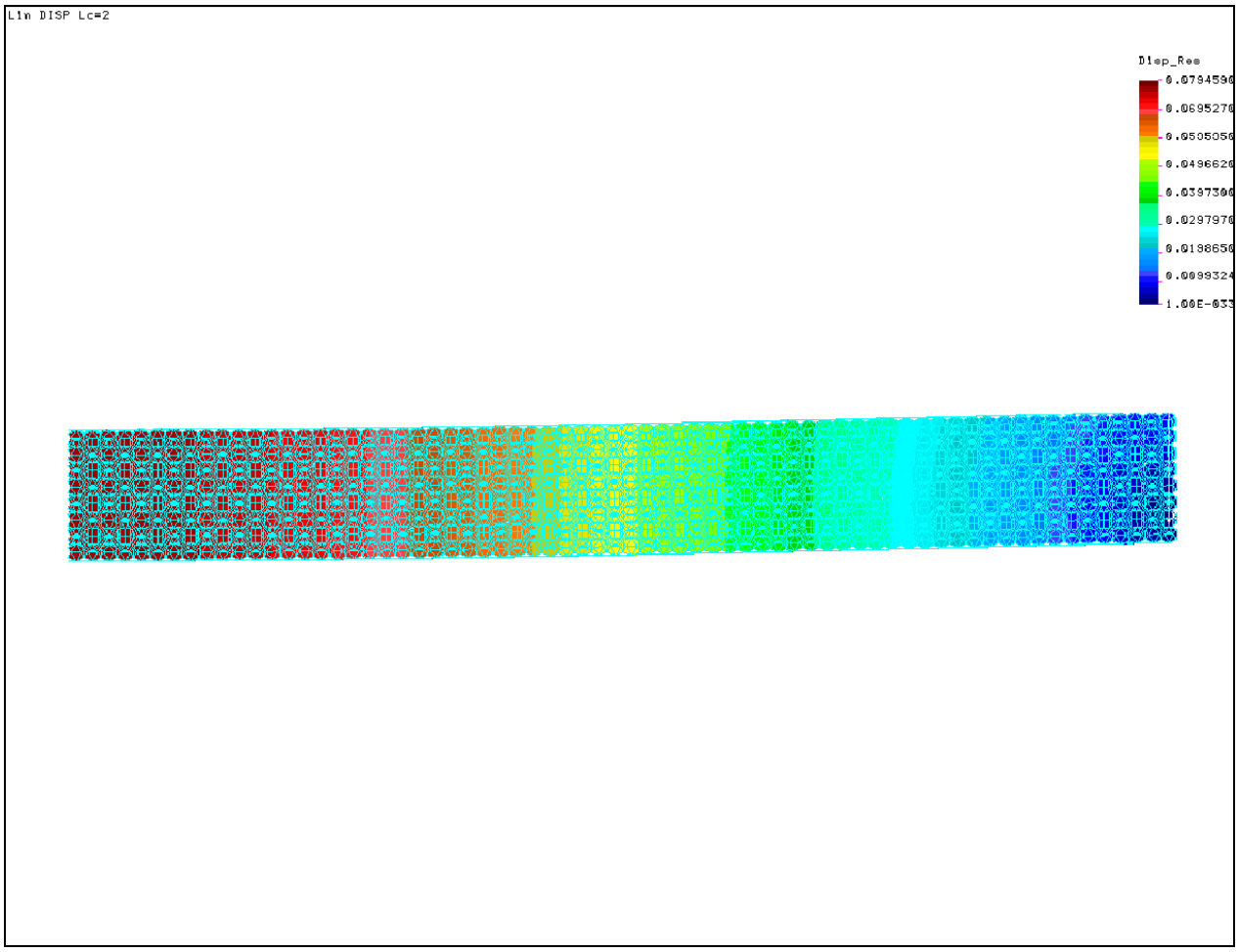


**Figure 16 Plot of Predicted Deflection - Strong Axis**

The Figure above shows a plot of the predicted deflection in strong axis bending. The deflection is less than that of the nominal wood beam.



ROSS ENGINEERING P.O. Box 65322 University Place, WA 98464-1322

## References:

**Machinery's Handbook**, Erik Oberg, Franklin D. Jones, and Holbrook L. Horton, 23rd Edition, Industrial Press Inc., New York, 1988
Referred to as: "***Machinery's Handbook***"

**Mark's Handbook for Mechanical Engineers, 8th Edition**, McGraw-Hill, 1989.
Referred to as: "***Mark's***"

**Mechanical Engineering Design**, Joseph E. Shigley and Charles R. Mischke, Fifth Edition, McGraw-Hill Book Company, 1989
Referred to as: "***Shigley***"

**Roark's Formulas for Stress and Strain**, Warren C. Young, Sixth Edition, McGraw-Hill Book Company, 1989
Referred to as: "***Roark's***"

**Uniform Building Code**, International Conference of Building Officials, 1991 Edition
Referred to as: "***UBC 1991***"

**Engineering Data for Aluminum Structures**, The Aluminum Association, Inc., Fifth Edition, 1986
Referred to as: "***Aluminum Data***"

**Specifications for Aluminum Structures**, The Aluminum Association, Inc. Fifth Edition, 1986
Referred to as: "Aluminum Structures"



ROSS ENGINEERING P.O. Box 65322 University Place, WA 98464-1322